

## CHAPTER NINETY

### A Laboratory Experiment of Beach Cusps

Arata Kaneko\*

Beach cusps with a longshore spacing of 20 to 150 cm have been built by the continuous action of incident waves on a steep laboratory beach. In the formation stage of beach cusps, all bed materials on the beach moved shoreward. The backwash vortex, which was found first by Matsunaga and Honji (16,18) on a laboratory beach, gave a good explanation of the shoreward movement of bed materials. Beach cusps formed when the value of a dimensionless parameter  $H_b^2 L_b / h_b^2 L$ , which controls swash motion on a steep beach, became larger than 1.12;  $H_b$  is the height of the breaking wave,  $L_b$  its wavelength,  $h_b$  the water depth at the breaking point and  $L$  the horizontal distance from the shoreline for still water level to the breaking point. The observational spacing of beach cusps formed regularly were in quite good agreement with half a wavelength of the zero-mode subharmonic edge wave generated on a sloping flat beach. As a result of this study, the contribution of edge waves on cusp formation becomes more undoubted.

#### Introduction

Beach cusps have been known as a prominent sedimentary feature on beaches with a quasi-uniform longshore spacing less than several tens meter. Since the first extensive field observation of Shepard (20), many works have been attempted to clarify the dynamics of beach cusps. Although there is still some controversy as to the cause of beach cusps (12), it seems natural to relate their formation to edge waves which generate on a beach and have a longshore periodicity. Also recent field observations provide evidence that shows the close correlation between beach cusps and edge waves (5,6,8,11,19).

In this study, beach cusps are observed in detail through each stage of formation on a steep laboratory beach. Vortices generated on the beach by swash motion are visualized and the vortex-induced mass transport flows are related to cusp formation. The criterion controlling cusp formation and the role of edge waves in the formation are also examined.

\* Associate Professor, Research Institute for Applied Mechanics, Kyushu University 87, Kasuga, Fukuoka 816, Japan.

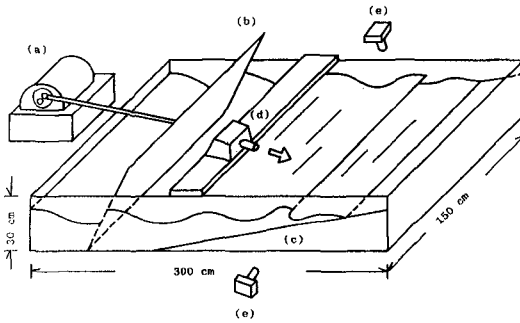


Figure 1. Sketch of experimental set-up:  
 (a) motor; (b) wave generator;  
 (c) model beach; (d) projector;  
 (e) camera.

### Experiments

Experiments were carried out using a wave tank 300 cm long, 150 cm wide and 30 cm deep, equipped with a beach floor 200 cm long (Fig.1). The side walls of the tank were made of transparent plastic to enable observation of bed features and flows on the beach floor. Incident waves on the model beach were formed by oscillating a wave-paddle-type generator with a motor-crank system. The beach slope ( $s$ ) and the period of incident waves ( $T_1$ ) were adjustable in the range of 0.081–0.141 and 0.5–2.4 s, respectively. Glass beads of mean diameter ( $D$ ) 0.028 cm and density ( $\rho_s$ )  $2.43 \text{ g cm}^{-3}$  were used as an erodible bed material instead of natural sands. In the experiment of cusp formation, the beach floor was initially covered with a thin bed of glass beads. The surface of the floor was also painted black to view clearly the movement of glass beads against the dark background. The direction of mass transport flow close to the bed could be estimated by following the movement of glass beads on the beach. Flow visualization was made by tracing the paths of polystyrene beads of  $D=0.15 \text{ cm}$  and  $\rho_s=1.04 \text{ g cm}^{-3}$ , which were suspended in water from the bed by the action of breaking waves. The bed surface and a vertical slice of the flow field were illuminated with a 1-kw light projector and photographed by a 35-mm camera from the positions shown in Fig.1.

### Formation of Cusps

When surface waves climb on a steep beach, the wave steepness increases continuously with the growth of the wave-height and the sharpened water surfaces break down rapidly at a short distance from the shore. We shall define the breaking point as the position where the

height of waves climbing on a beach becomes maximum and the plunging point as the position where the forward face of breaking waves impinges on the water surface ahead. For convenience, we shall use the terms offshore and nearshore zone, respectively, for the seaward and the shoreward sides of a breaking point. The nearshore zone is further divided into breaker and swash zones at a plunging point. It should be noted that no surf zone exists on a steep beach. In all photographs presented later, the right-hand direction indicates shoreward.

Figure 2 shows the formation process of typical beach cusps formed at the condition of  $s=0.081$ ,  $T_1=1.15$  s,  $H_b=3.5$  cm and  $h_b=4.0$  cm, where  $H_b$  is the height of breaking waves and  $h_b$  the water depth at a breaking point. Photographs were taken obliquely over a side wall of the tank after the wave generator was stopped temporarily at each stage of cusp formation. Figure 2a shows the initial feature of the glass-bead bed with 0.2 cm thick over the nearshore zone of 49 cm wide. A dotted line indicates the shoreline for still water level, and a bar at top right is 10 cm. After breaking waves begin to attack the beach, all glass beads gradually move shoreward forming a sedimentary zone parallel to the shore just at the seaward side of the plunging point (Fig.2b). As a result, the amounts of glass beads piled up on the beach face increases continuously. The sedimentary zone begins to diminish with decrease of offshore glass beads, and the ridge of glass beads on the beach face becomes cut by a series of narrow channels equi-spaced in the longshore direction. Finally a clear ridge-channel system, as seen in Fig.2c, forms. The run-up length of water becomes maximum at the central point of the ridges and minimum at the channels. Therefore, water running up on the ridges turns back along the channels, forming strong rip currents. The geometry of the ridge-channel system and the pattern of water circulation are sketched in Fig.3. The same bed and

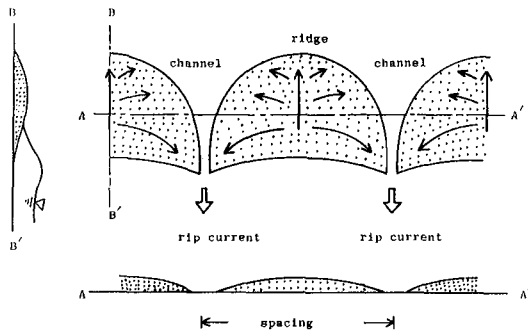


Figure 3. Sketch of the ridge-channel system. The bed profiles of sections A-A' and B-B' are presented at the lower and the left parts, respectively.

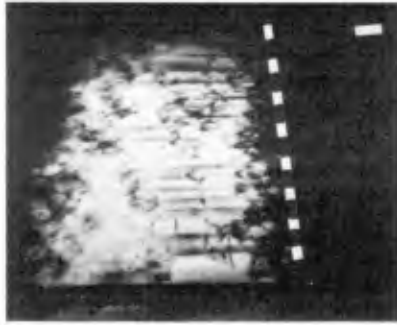
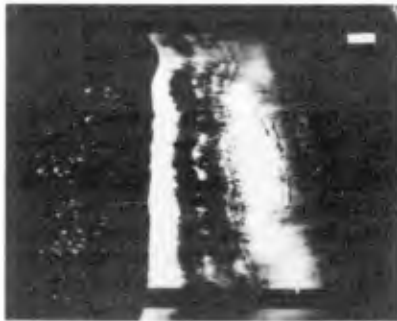
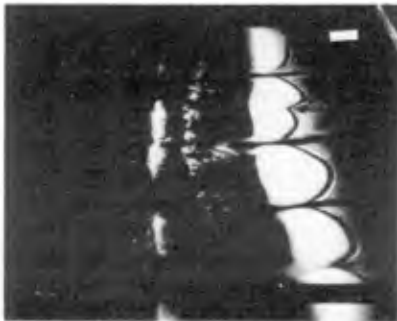
(a)  $t = 0$  s(b)  $t = 223$  s(c)  $t = 784$  s

Figure 2. Formation process of typical beach cusps.  
 $t$  denotes the elapsed time from the start of the experiment.

flow features have often been observed in wave tanks (17,21). In the field, Sallenger (19) observed that a similar ridge-channel system generated in flood-tide changes to ordinary beach cusps after the mouth of the channels was eroded widely on ebb-tide. It will, therefore, be reasonable to call such a ridge-channel system the beach cusp. Kaneko (9) showed through a numerical experiment that horizontal circulation systems are induced by the nonlinear effect of swash motion due to edge waves. This circulation may also play a role in the initiation of beach cusps.

#### Flows on a Steep Beach

Figure 4 shows the anticlockwise-rotating vortex induced near a plunging point immediately after breaking waves forming beach cusps impinged on the forward water surface just beneath a horizontal scale of 4 cm. The experimental condition was at  $s=0.081$ ,  $T_i=1.68$  s,  $H_b=3.7$  cm and  $h_b=3.9$  cm. The vertical slice at a distance of 10 cm from a side wall was illuminated by a light projector and photographed through the side wall. This vortex, called the backwash vortex, was first found by Matsunaga and Honji (16) to form on a highly steep beach in a wave tank. The backwash from water running up on a beach face is responsible for the vortex formation. The backwash vortex is also known to make up a step-like bed profile, composed of a steep seaward face and a nearly horizontal top and called the backwash step (16). Taking into account flow fields induced by the backwash vortex, we can sketch the overall pattern of mass transport flow forming beach cusps and a backwash step, as in Fig.5. The piling-up of bed materials on the beach face, as seen in Fig.2, can also be well explained by the vortex-induced mass transport flow. The wave-induced mass transport flow of Longuet-Higgins (13) may play a role in the shoreward transport of offshore sands.

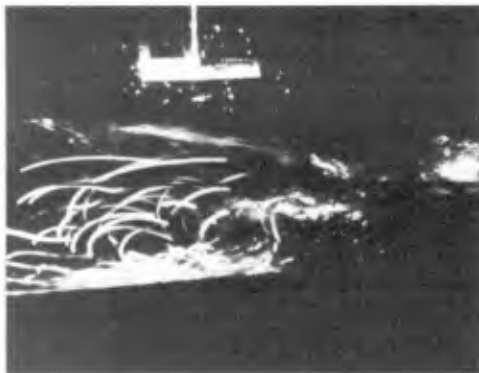


Figure 4. Flows beneath the breaking wave forming beach cusps.

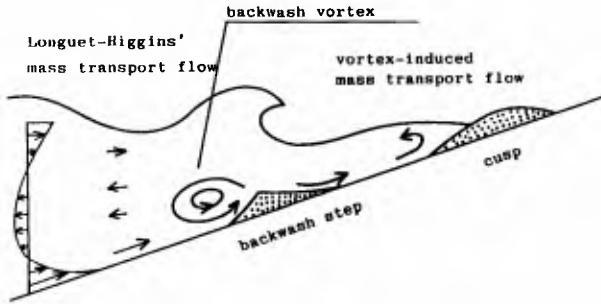


Figure 5. Sketch of mass transport flow forming beach cusps and a backwash step.

Figure 6 shows the flow field near a plunging point photographed immediately after breaking waves forming a longshore bar impinged on the forward water surface just beneath a horizontal scale of 4 cm. The method of photography and light projection was the same as in Fig.4. The experimental condition was at  $s=0.081$ ,  $T_i=0.62$  s,  $H_b=3.3$  cm and  $h_b=4.3$  cm. Notice that  $T_i$  is remarkably reduced in comparison with that for Fig.4. Under such a condition, the period of breaking waves became shorter than that of swash motion. As a result, weak swash motion and prominent wave set-up took place. Flows near the plunging point construct a pair of vortices, a clockwise, shoreward vortex and an anticlockwise, seaward one. The paired vortex may be induced by that the wave-induced mass transport flow of Longuet-Higgins (13) and the undertow due to wave set-up proposed by Longuet-Higgins(15) meet near the plunging point. The longshore bar was observed to form on the bed between these vortices (10). We can also sketch the overall pattern of mass transport flow forming a longshore bar, as in Fig.7.

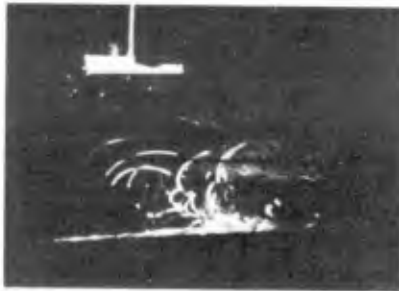


Figure 6. Flows beneath the breaking wave forming a longshore bar.

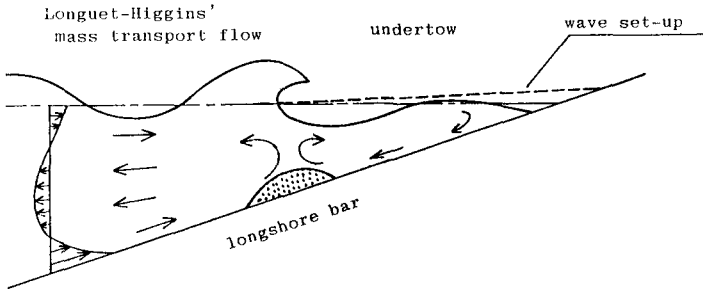


Figure 7. Sketch of mass transport flow forming a longshore bar.

Criterion for Cusps

In the present experiment, beach cusps developed from a thin glass-bead bed on a beach floor. Because of the small amount of glass beads used, the resulting bed deformation could not grow sufficiently to change the initial conditions of incident waves, the height of breaking waves and the breaking point. Under such a situation, the formation region of beach cusps may be determined by the wave conditions on a rigid plane beach.

As mentioned in the previous section, the backwash vortex generated by strong swash motion is responsible for the movement of bed materials to form beach cusps. We shall analyse the swash motion on a steep beach, making use of the terminology as sketched in fig.8. Let  $L_r$  and  $L$  denote the run-up length and the horizontal distance from a shoreline for still water level to a breaking point, respectively.

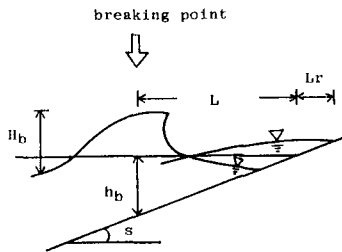


Figure 8. Sketch of the swash motion on a steep beach.

When we simulate a breaking wave by a progressive long wave with wave-height  $H_b$  and wavelength  $L_b$ , its energy over a wavelength may be estimated as proportional to  $\rho g H_b^2 L_b$ , where  $L_b = T_i \sqrt{g h_b}$ . We also simulate swash motion by a standing wave with maximum wave-height  $2L_r s$  at a shoreline for still water level and estimate its energy over a nearshore zone as proportional to  $\rho g (L_r s)^2 L$ . Since a part of energy of the breaking wave is transferred to the swash motion, both the energies may be correlated as follows:

$$\rho g H_b^2 L_b \propto \rho g (L_r s)^2 L \tag{1}$$

Rearranging eq.1 and using  $h_b = sL$ , we can obtain the following relation:

$$\frac{L_r}{L} \propto \left( \frac{H_b^2 L_b}{h_b^2 L} \right)^{1/2} \tag{2}$$

The observational values of  $L_r/L$  are plotted in Fig.9 against those of  $H_b^2 L_b / h_b^2 L$ . In Fig.9, the line for eq.2

$$\frac{L_r}{L} = 0.35 \left( \frac{H_b^2 L_b}{h_b^2 L} \right)^{1/2} \tag{3}$$

best fitting into the plotted data is also drawn. The dimensionless parameter  $H_b^2 L_b / h_b^2 L$  controlling swash motion on a steep beach is called the swash parameter here. Some deviation of the plotted data from eq.3 seems due to that the energy transferred to nearshore mass transport flow and wave set-up are neglected in this analysis. The deviation at the region of large  $H_b^2 L_b / h_b^2 L$  may also be influenced by the excitation of edge waves. The swash parameter can be rewritten as:

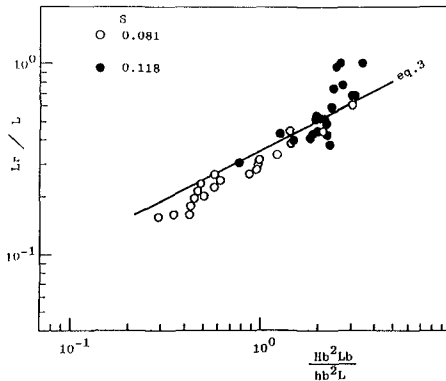


Figure 9. Run-up length.

$$\frac{H_b^2 L_b}{h_b^2 L} = \left(\frac{H_b}{s^2 g T_1^2}\right)^{-1/2} \left(\frac{H_b}{h_b}\right)^{5/2} \tag{4}$$

The values of  $H_b/h_b$  for the present experiment are plotted in Fig.10 against those of  $(H_b/s^2 g T_1^2)^{1/2}$ . Most of the plotted data are grouped by the critical line

$$\frac{H_b^2 L_b}{h_b^2 L} = 1.12 \tag{5}$$

or

$$\left(\frac{H_b}{h_b}\right)^{5/2} = 1.12 \left(\frac{H_b}{s^2 g T_1^2}\right)^{1/2} \tag{5}'$$

into two regions of the beach cusp and the longshore bar, where the dimensionless parameter  $(H_b/s^2 g T_1^2)^{1/2}$  has been called the surf similarity parameter by Battjes (2). According to Battjes' study, the generation regions for surging, plunging and spilling breakers are, respectively,  $(H_b/s^2 g T_1^2)^{1/2} < 0.2$ ,  $0.2 < (H_b/s^2 g T_1^2)^{1/2} < 1.0$  and  $1.0 < (H_b/s^2 g T_1^2)^{1/2}$ . It should be noted that the beach cusp is transferred to the longshore bar at a nearly central part of the generation region for plunging breakers.

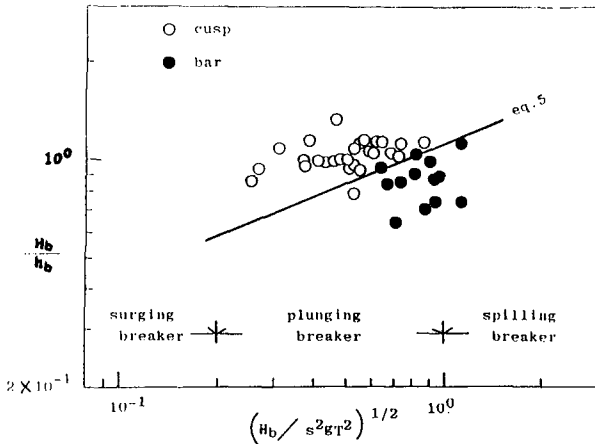


Figure 10. Formation region of cusps.

## Edge waves

According to Ursell's theory (24), the wavelength of edge waves ( $L_e$ ) can be expressed as:

$$L_e = gT_e^2 \sin \{(2n+1)s\} / 2\pi \quad (6)$$

where  $T_e$  and  $n$  are the period and the offshore modal number of the edge wave, respectively. Edge waves on a beach may be classified into two types of subharmonic and synchronous depending on whether the period of edge waves is twice or the same as that of incident waves. Guza and Davis (4) predicted theoretically that the zero-mode ( $n=0$ ) subharmonic edge wave can most easily be excited by incident waves. Huntley and Bowen (7) and Guza and Bowen (6) also found that in the power spectra of nearshore currents, the zero-mode subharmonic edge wave takes place on real beaches. When the longshore undulation of small amplitude due to edge waves is superimposed on the uniform swash motion due to incident waves, the compound swash motion is known to have the longshore spacing of half a wavelength of subharmonic edge waves or a wavelength of synchronous ones (3,10). Equating the spacing of swash motion and beach cusps and using eq.6 and  $T_i$  instead of  $T_e$ , we can express the calculated spacing of cusps ( $L_{cal}$ ) as:

$$L_{cal} = L_e/2 = gT_i^2(\sin s)/\pi \quad (7)$$

for the zero-mode subharmonic edge wave and:

$$L_{cal} = L_e = gT_i^2(\sin s)/2\pi \quad (8)$$

for the zero-mode synchronous edge wave.

Other examples of beach cusps formed regularly are showed in Figs.11a to e. In all the figures, a bar at top right is 10 cm.



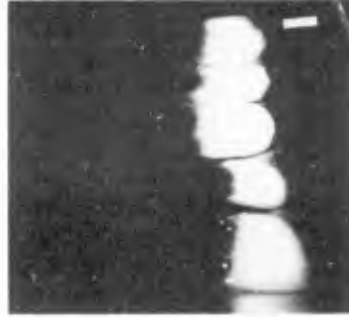
(a)



(b)



(c)



(d)



(e)

Figure 11. Five examples of beach cusps formed regularly.

Similarly to Fig.2, these beach cusps are composed of ridge-channel systems. Using the width of the wave tank ( $B$ ) and the total number of the ridges ( $N$ ), we can obtain the observational spacing of cusps ( $L_{\text{Obs}}$ ) as:

$$L_{\text{Obs}} = \frac{B}{N - 1} \quad (9)$$

The numerical data of these beach cusps are presented in Table 1. The value of  $L_{\text{Obs}}$  is in quite good agreement with that of  $L_{\text{Cal}}$  based on subharmonic edge waves. It seems that beach cusps become regular when the resonance condition of zero-mode subharmonic edge waves is satisfied with good accuracy. If edge waves occur on a beach, it will be expectable to find them in the longshore undulation of swash motion.

Table 1. Numerical data of beach cusps formed regularly.

Fig.11	s	T <sub>i</sub> (s)	H <sub>b</sub> (cm)	h <sub>b</sub> (cm)	$\frac{H_b^2 L_b}{h_b^2 L}$	L <sub>cal</sub> (cm)	L <sub>obs</sub> (cm)
a	0.081	2.38	3.4	3.1	4.08	143	150
b	0.081	1.72	3.1	3.1	2.42	74	75
c	0.141	0.98	4.2	3.2	4.30	42	38
d	0.107	0.98	3.4	2.9	2.85	32	30
e	0.107	0.76	3.5	3.1	2.20	19	21

Such a property of swash motion was visible only in the experiment for Figs.11a and b with the large cusp spacings. In other cases, edge waves excited may be too weak to be found in swash motion. The values of L<sub>obs</sub> for the laboratory experiments of Ann (1), Tamai (22) and the author, and the field observations of Longuet-Higgins and Parkin (14), Komar (11), Sallenger (19), Guza and Bowen (6) and Takeda and Sunamura (23) are plotted in Fig.12 against that of  $gT_i^2(\sin s)/\pi$ . The value of L<sub>cal</sub> for subharmonic and synchronous edge waves are also drawn with solid and dotted lines, respectively. Although all the laboratory data and most of the field data have a best fit with the solid line, there are some data of Longuet-Higgins and Parkin, Komar and Sallenger which show a scatter around the dotted line. The critical condition, at which synchronous edge waves are transferred to subharmonic ones, may exist.

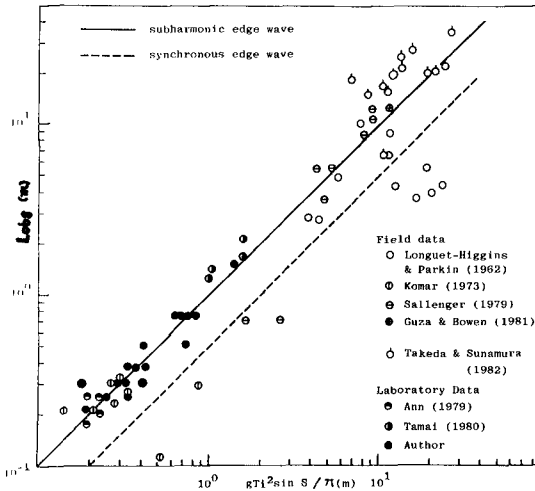


Figure 12. Spacing of cusps.

## Conclusions

Main results obtained in the present study are summarized as follows:

- (1) Beach cusps develop at the beach face when all bed materials on a beach move shoreward, forming a backwash step along the plunging point.
- (2) When all bed materials on a beach assemble near the plunging point, beach cusps can not develop and instead a longshore bar forms along this point.
- (3) Vortices induced beneath the breaking waves by the action of swash motion or wave set-up control the movement of bed materials at the swash zone.
- (4) The transition from the beach cusp to the longshore bar takes place at  $H_b^2 L_b / h_b^2 L = 1.12$ . This dimensionless parameter controlling swash motion on a steep beach is called the swash parameter.
- (5) The observational spacing of beach cusps obtained in the laboratory experiment agrees well with half a wavelength of the zero-mode subharmonic edge wave. A relatively large scatter of the field data may be explained consistently by considering the existence of beach cusps generated by the zero-mode synchronous edge wave.

## Acknowledgments

I would like to thank Prof. H. Honji for valuable suggestions and criticism and Mr. Y. Shiraishi for technical assistance.

## References

1. Ann, K., Experimental study on the formation of rhythmic shorelines, Unpublished Master's Thesis, University of Tokyo, Tokyo, in Japanese, 1979, p.1-135.
2. Battjes, J.A., Surf similarity, Proc. 14th Conf. Coastal Eng., Copenhagen, 1974, p.466-480.
3. Bowen, A.J., Edge waves and the littoral environment, Proc. 13th Conf. Coastal Eng., London, 1972, p.1313-1319.
4. Guza, R.T. and Davis, R.E., Excitation of edge waves by waves incident on a beach, J. Geophys. Res., 79, 1974, p.1285-1291.
5. Guza, R.T. and Inman, D.L., Edge waves and beach cusps, J. Geophys. Res., 80, 1975, p.2997-3012.
6. Guza, R.T. and Bowen, A.J., On the amplitude of beach cusps, J. Geophys. Res., 86, 1981, p.4125-4132.
7. Huntley, D.A. and Bowen, A.J., Field observations of edge waves, Nature, 243, 1973, p.160-162.
8. Inman, D.L. and Guza, R.T., The origin of swash cusps on beaches, Mar. Geol., 49, 1982, p.133-148.
9. Kaneko, A., A numerical experiment on nearshore circulation in standing edge waves, Coastal Eng., 7, 1983, p. 271-284.
10. Kaneko, A., Formation of beach cusps in a wave tank, Coastal Eng., in press, 1985.
11. Komar, P.D., Observations of beach cusps at Mono Lake, California, Geol. Soc. Am. Bull., 84, 1973, p.3593-3600.

12. Komar, P. D., Beach Processes and sedimentation, Prentice-Hall, Englewood-Cliffs, N. J., 1976, p.263-274.
13. Longuet-Higgins, M. S., Mass transport in water waves, Philos. Trans. R. Soc. London, A245, 1953, p.535-581.
14. Longuet-Higgins, M. S. and Parkin, D. W., Sea waves and beach cusps, Geogr. J., 128, 1962, p.194-201.
15. Longuet-Higgins, M. S., Wave set-up, percolation and undertow in the surf zone, Proc. R. Soc. London, A390, 1983, p.283-291.
16. Matsunaga, N. and Honji, H., The backwash vortex, J. Fluid Mech., 99, 1980, p.813-815.
17. Matsunaga, N. and Honji, H., A petaline sand pattern along the shoreline, Rep. Res. Inst. Appl. Mech., 29, 1981, p.1-12.
18. Matsunaga, N. and Honji, H., The steady and unsteady backwash vortices, J. Fluid Mech., 99, 1983, p.189-197.
19. Sallenger, A. H., Beach-cusp formation, Mar. Geol., 29, 1979, p. 23-37.
20. Shepard, F. P., Gravel cusps on the California coast related to tides, Science, 82, 1935, p.251-253.
21. Tamai, S., Study on the formation of beach cusps, Proc. 21st Japanese Conf. Coastal Eng., Sendai, 1974, in japanese, p.115-120.
22. Tamai, S., Study on the characteristics of beach cusps and the prediction of shoreline changes, Doctor's Dissertation, Kyoto University, Kyoto, 1980, in japanese, p.1-179.
23. Takeda, I. and Sunamura, T., Formation and wavelength of beach cusps, Proc. 29th Japanese Conf. Coastal Eng., Sendai, 1982, in japanese, p.319-322.
24. Ursell, F., Edge waves on a sloping beach, Proc. R. Soc. London, A214, 1952, p.79-97.